Journal of Applied Polymer Science

Interactions in blends of dendronized polymeric nanocomposites with some common drugs

Nancy Alvarado,[1] Irma Fuentes,[1] Luz Alegría,[2] Claudia Sandoval,[3] Galder Kortabería,[4] Arantxa Eceiza,[4] Ligia Gargallo,[5] Angel Leiva,[1] Deodato Radić[1]

[1]Depto Química Fisica, Facultad de Química, Pontificia Universidad Católica de Chile, Casilla 306, Santiago, Chile
[2]Centro de Docencia de Ciencias Básicas para Ingeniería, Facultad de Ciencias de la Ingeniería, Universidad Austral de Chile, Casilla 567, Valdivia, Chile
[3]Universidad Autónoma de Chile, Instituto de Ciencias Químicas Aplicadas, El Llano Subercaseaux 2801, San Miguel, Santiago, Chile
[4]Group "Material+Technologies," Dept Ingeniería Química y M. Ambiente, Escuela Politécnica, Universidad País Vasco/Euskal Herriko Unibersitatea, Pza Europa 1, 20018 Donostia, San Sebastián España
[5]Universidad de Tarapacá, General Velásquez 1775, Arica, Chile
Correspondence to: D. Radić (E-mail. dradic@puc.cl)

ABSTRACT: Poly(diethylaminoethyl methacrylamide) (PEAM), a dendronized polymer, was synthesized according to classical procedures. Monomers and polymers were characterized by spectroscopic measurements. The results obtained were in agreement with the expected chemical structure. The phase behavior of blends of PEAM with diclofenac (DCF), ibuprofen (IBU), and paracetamol (PCM) were studied by different experimental techniques. FT-IR, UV-Vis, DSC, and TGA measurements suggested important interactions between the blended components. Thermogravimetric analysis (TGA) indicated the temperature at which the dendronized polymer released a small molecule. AFM measurements and molecular dynamics (MD) simulations were used to better understand the nature of the interactions and to estimate the distance between the components of the blends to explain the interaction involved.
 J. Appl. Polym. Sci. **2015**, *132*, 42450.

KEYWORDS: blends; compatibilization; dendrimers; hyperbranched polymers and macrocycles; structure-property relations; theory and modeling

Received 13 January 2015; accepted 30 April 2015
DOI: 10.1002/app.42450

INTRODUCTION

Dendronized polymers are a special family of polymers in which the side chain is composed of a dendritic structure with different conformational arrangements. This chemical structure gives rise to a special property of the macromolecule, and its behavior is interesting for various reasons. Low molecular weight molecules are often used as carriers and to prepare new compounds, including pharmaceutical compounds, dyes, catalysts, etc. In contrast, macromolecules with large molecular weights are used directly in industry. The most significant difference between small and large molecules is that macromolecules, unlike small molecules, do not have a specific shape and therefore lack predictable properties.[1–8] For instance, the diameter of the polymers can be changed by changing their physical environment. Investigations of intermediate-sized nanoscale molecules with specific shapes and functionalities along with well-defined molecular weights are interesting. These molecules can be nonlinear oligomeric units called dendrimers. However, such molecules are able to receive small molecules as guests and can be used as a delivery systems for drugs, catalysts, dyes, etc.[9–11] Such systems can be considered a special type of polymer blend, where the interactions between the polymer and the small molecules should determine the general behavior of the mixture and the rate of release of the small molecules. This special type of mixture should be considered in the development of a model to suggest a mechanism for the delivery of small molecules and to take advantage of the type of interactions involved in the blend process. Previously, the elucidation of such mechanisms required knowledge of the particular behavior of the polymer-small molecule pair.

Polymer blends are a subject of current interest because the various methods of blending enable the creation of materials with new and enhanced properties;[12] however, the behavior of polymer-small molecule blends differs from that of polymer-polymer blends. These new types of polymeric materials can be analyzed by the same experimental techniques used to analyze

polymer-polymer blends, i.e., DSC, TGA, FT-IR, UV-Vis, AFM, etc.

The aim of the present work is to study the interactions within blends containing an interacting dendronized polymer, i.e., poly(diethylaminoethyl methacrylamide) (PEAM), with some common drugs such as ibuprofen (IBU), diclofenac sodium salt (DCF), paracetamol (PCM) (see Scheme 1). Using this approach, we determined the effect of the functionalization of the small molecule on the releasing mechanism and obtained information about the interactions involved in such systems.

EXPERIMENTAL

Materials Synthesis and Chain Characterization

All reagents and solvents were purchased from Sigma-Aldrich. Diethylaminoethyl methacrylamide was obtained by reaction of methacryloyl chloride and 2-*N*,*N*-diethylamine in the presence of triethylamine at room temperature according to the previously reported procedure.[13] The monomer EAM was polymerized in bulk using α,α′-azobisisobutyronitrile (AIBN) (0.5% wt) as the initiator under previously dried N2 atmosphere. Polymerization was carried out in bulk at 65°C for 48 h ($M_w = 52{,}700$ (g/mol), DPI = 1,2).[13]

Spectroscopic Characterization

Proton nuclear magnetic resonance (^{1}H-NMR) spectra were collected on a Bruker ACP Avance-400 spectrometer at 400 MHz; the samples were dissolved in $CDCl_3$, and tetramethylsilane was used as an internal standard for EAM and PEAM.[13]

FT-IR spectra were recorded on a Bruker Vector 22 spectrophotometer using KBr pellets; the spectra were collected at a resolution of 1 cm^{-1}. UV-Vis measurements of the pure components and blends were recorded on an Agilent Technologies CARY 60 UV-Vis spectrophotometer; the samples were dissolved in methanol at concentrations of 4.5×10^{-3} mg/mL to 1.6×10^{-3} mg/mL, and their absorbance was measured at wavelengths between 350 and 200 nm. UV-Vis PEAM/PCM spectra were deconvoluted and then curve-fitted with Gaussian bands using ORIGIN PRO 9.0 software.

Molecular Characterization

Weight-average molecular weight (M_w) and polydispersity (M_w/M_n) values of the polymer were determined using a Viscotek (VE 1122 solvent delivery system) size exclusion chromatograph equipped with a VE 3580 RI refractive index detector. The mobile phase was chloroform ($CHCl_3$), and separation was carried out with a T600M column. An elution rate of 1 mL/min at 30°C and 1 wt % solutions of the polymer in $CHCl_3$ were used. The molecular weight distribution was calculated on the basis of a calibration curve constructed using monodisperse poly(styrene) standards.[13]

Blends Preparation

Films were obtained by dissolving each polymer separately (2 wt % solution) in $CHCl_3$. Solutions were then mixed, and the blends were stirred for 24 h. The blends were then dried under

Table I. Glass-Transition Temperatures, T_g (°C), for Blends of PEAM/IBU, PEAM/DCF, and PEAM/PCM at Different Compositions and Melting Temperatures, T_m (°C), for IBU, DCF, and PCM

	Composition (wt %)						
	0	20	40	50	60	80	100
	T_g (°C)						T_m (°C)
IBU	90	101	89	91	97	95	77
DCF	90	92	85	-	115	130	267
PCM	90	93	87	89	98	95	158

vacuum at 25°C to a constant weight. The drugs used for the blends were DCF, IBU, and PCM (Scheme 1).

Thermal Analysis

TGA was carried out on a Mettler Toledo TGA/SDTA 851. The scans were performed at temperatures ranging from 25°C to 700°C at a heating rate of 10°/min under a dry nitrogen atmosphere. The sample masses were 5 to 10 mg, and the samples were placed in 40 μL alumina pans. Data were processed using the STAR^e software version 8.1 from Mettler-Toledo. The thermal transitions of the polymer were studied by DSC on a Mettler-Toledo DSC 821-700 differential scanning calorimeter; the samples were measured under dry nitrogen and at a heating rate of 10°C/min. The thermal curves of the samples were obtained using the following heating method: a 5 min hold at 300°C, a decrease temperature to −100°C at 10°/min, a 2-min hold at −100°C and an increase in temperature to 300°C at 10°/min. The second heating cycle was used for analysis. Data obtained were processed using the STAR^e software version 8.1 from Mettler-Toledo.

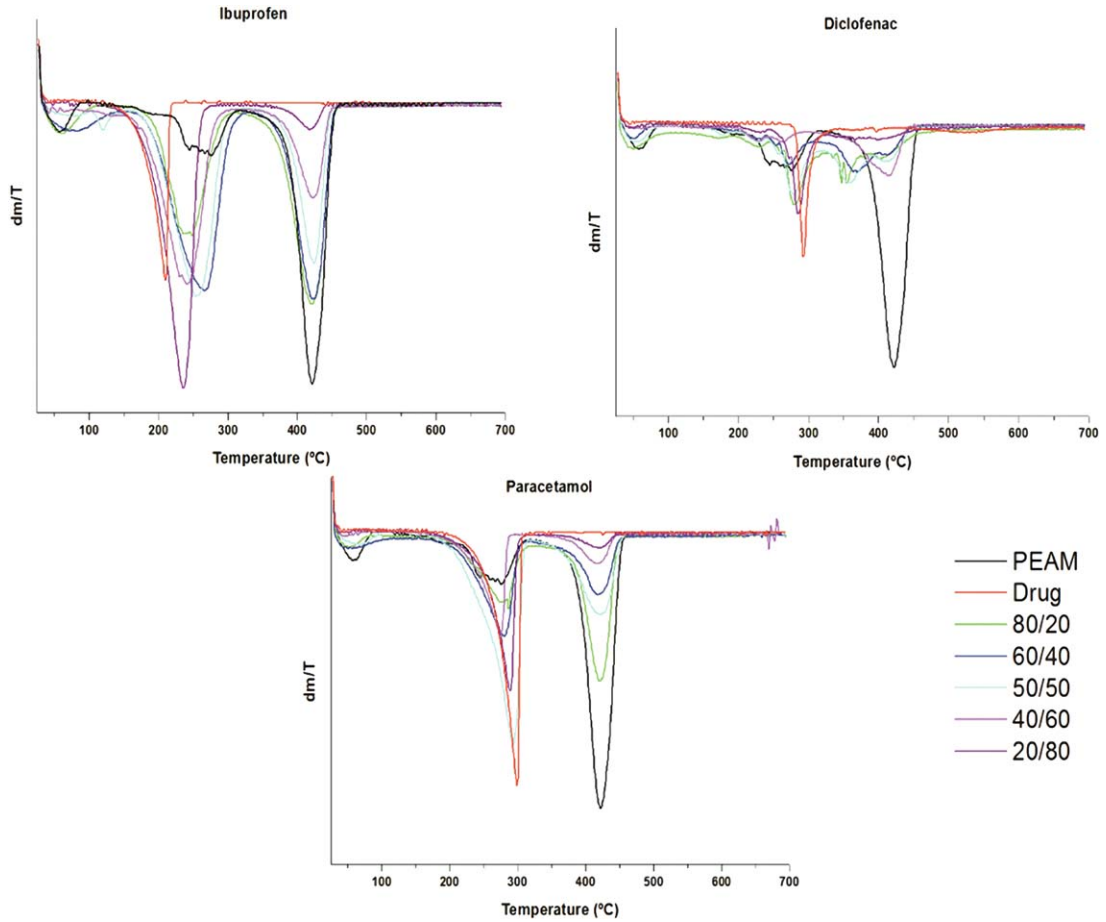

Figure 1. TGA thermograms of a) PEAM/IBU: (1) PEAM, (2) IBU, (3) IBU 20%, (4) IBU 40%, (5) IBU 50%, (6) IBU 60%, and (7) IBU 80%; b) PEAM/DCF: (1) PEAM, (2) DCF, (3) DCF 20%, (4) DCF 40%, (5) DCF 50%, (6) DCF 60%, and (7) DCF 80%; c) PEAM/PCM: (1) PEAM, (2) PCM, (3) PCM 20%, (4) PCM 40%, (5) PCM 50%, (6) PCM 60%, and (7) PCM 80%. [Color figure can be viewed in the online issue, which is available at wileyonlinelibrary.com.]

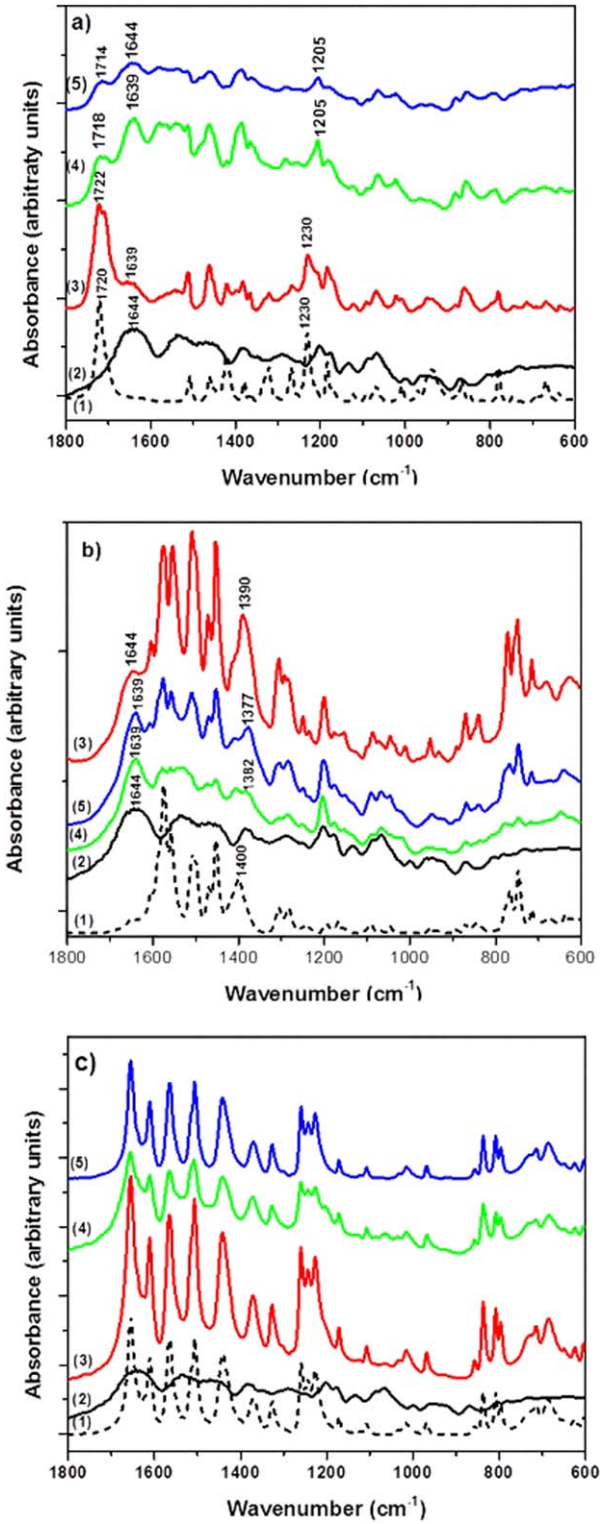

Figure 2. FT-IR spectra of a) PEAM/IBU: (1) PEAM, (2) IBU, (3) IBU 20%, (4) IBU 40%, (5) IBU 50%, (6) IBU 60%, and (7) IBU 80%; b) PEAM/DCF: (1) PEAM, (2) DCF, (3) DCF 20%, (4) DCF 40%, (5) DCF 50%, (6) DCF 60%, and (7) DCF 80%; c) PEAM/PCM: (1) PEAM, (2) PCM, (3) PCM 20%, (4) PCM 40%, (5) PCM 50%, (6) PCM 60%, and (7) PCM 80%. Black (dotted), drug; red, 20 wt %; green, 40 wt %; blue, 50 wt %; black, PEAM. [Color figure can be viewed in the online issue, which is available at wileyonlinelibrary.com.]

Atomic Force Microscopy

AFM images were obtained in tapping mode with a Nanoscope IIIa Multimode® scanning probe microscope from Digital Instruments, Veeco. Commercial Si cantilevers with force constants of 20 to 80 N/m were used. Samples were prepared by spin-coating at 2000 rpm for 60 s using a Telstar Instruments model P-6708D spin-coater. The blend solutions (0.1–0.2 wt % in $CHCl_3$) were coated onto cleaved glass substrates.

Molecular Dynamics Simulation

The initial structures for each polymer fragment used in this study were constructed with 10 repeating units for each polymer using the Materials Studio software. The fragments were minimized and equilibrated through a molecular dynamics (MD) simulation. The initial configuration of the systems was optimized using the "smart minimizer" method, which is a minimization protocol implemented in the Discover module. Three minimization methods were used: Steepest descent, Conjugate gradient, and Newton methods. The equilibration and relaxation steps were a 1.0 ns MD simulation at 350 K using the Andersen thermostat in the NVT ensemble with a time step of 1.0 fs. Short-range electrostatic and van der Waals interactions were truncated at 9.5 Å. All MD simulations were performed using the Discover module of Materials Studio, and a PCFF force field was used for this purpose. The last conformation for each polymer fragment was saved and used to calculate the energy of blend between PEAM and the small molecules. The BLEND module of the Materials Studio software was used. PEAM was a screen fragment, whereas DCH_S, IBU, DCF, and PCM were the base fragments.

RESULTS AND DISCUSSION

Synthesis and Characterization of Monomers and Polymers

Functionalized poly(methacrylamide) was obtained by polymerization of the monomer through the reaction of 2-*N*,*N*-diethylethylamine and methacryloyl chloride. Radical polymerization was carried out with AIBN as the initiator, as previously reported[13] (Scheme 2). The monomer and the polymer were characterized by ^{1}H-NMR. Different signals were observed, corresponding to: monomer, 6.57 ppm (s, 1H; NH_2), 5.71 ppm (s, 1H; $=CH_2$), 5.30 ppm (s, 1H; $=CH_2$), 3.74 ppm (m, $J = 6.0$ Hz, 2H; CH_2), 3.34 ppm (dd, $J = 11.3$, 5.5 Hz, 2H; CH_2), 2.55 ppm (dt, $J = 14.2$, 6.5 Hz, 6H; CH_2), 1.98 ppm (m, 3H; CH_3), 1.01 ppm (s, 6H; CH_3). These signals are in agreement with the expected chemical structure for the monomer. The chemical shifts in the spectrum of the polymer were as follows: 7.26 ppm (s, 1H; NH_2), 3.46 ppm (m, 2H; CH_2), 1.67 ppm (m, 6H; CH_3), 1.35 ppm (m, 3H; CH_3), 0.9 ppm (m, 8H; CH_2). These signals are in agreement with the expected chemical structure of the polymer. The signals associated with the vinylic hydrogens of the monomer (at 5.25 and 5.75 ppm) disappeared, which is an important result for characterizing the polymer structure. The FT-IR spectra show the main absorption bands corresponding to the amide and carbonyl functional groups, together with the stretching vibrations corresponding to methyl and methylene groups; these bands are summarized as: 3440 cm^{-1} (—NH), 1644 cm^{-1} (—C=O amide) 2973 cm^{-1} (—CH_2) and 2933 (CH_3) cm^{-1}.

Table II. FT-IR Main Absorptions and Shifts of the Functional Groups Involved in the Polymer/Drug Interactions for a) PEAM/IBU, b) PEAM/DCF, and c) PEAM/PCM

a) PEAM/IBU					
Composition (wt %)	IBU	20	40	50	PEAM
Wavenumber (cm^{-1})	1720-1230	1722-1230	1718-1205	1714-1205	1644
b) PEAM/DCF	DCF	20	40	50	PEAM
Composition (wt %)					
Wavenumber (cm^{-1})	1400-1644	1390-1644	1382-1639	1377-1639	1644
c) PEAM/PCM	PCM	20	40	60	
Composition (wt %)					
Wavenumber (cm^{-1})	1638	3414-1638	3420-1638	3424-1638	1644

Thermal Analysis

The main criterion for miscibility of a material is the presence of a single glass-transition temperature (T_g), which should be intermediate between the T_g of the pure components.[14–16] Nevertheless, in the case of blends of polymers and small molecules, the melting point (T_m) of the small molecules disappears, which indicates that the polymer and the small molecules are part of the same structure. If the blend were immiscible, the T_g and T_m signals of the individual components would be observed.

Transparent films were obtained at room temperature. The PEAM/drug blends exhibit a single T_g over the whole range of compositions. The exception is the blend PEAM/DCF (50/50 wt %). The T_g and T_m values corresponding to the blends and drugs, respectively, are summarized in Table I.

Table I shows that, for blends containing ibuprofen, the T_g values were higher than the value for pure PEAM and that the highest value was reached when the composition of the drug is 20% wt. When the blend contained 80% wt of DCF, the T_g value of the blend reached the highest value of 130°C. For the blends containing PCM, the T_g variation exhibited a shape with values over and below the T_g of the pure polymer, reaching the higher value when the ibuprofen content was 60% wt (Table I); therefore, we presume that some type of affinity existed between the components.

The TGA profiles, represented as the first derivative (DTG = dm/dT), for different compositions of PEAM/drug blends are shown in Figure 1. All blends exhibited a similar trend, with two stages of decomposition. This decomposition profile was attributed to degradation of the polymer molecule in steps. The first step of the degradation was due to the disruption of the polymer-drug association and to the cleavage of the small molecule, consistent with the melting temperatures of the drugs. The second step corresponded to the degradation of the polymeric backbone. Therefore, this behavior suggested that the small molecules could be trapped inside the cavity of the dendronized polymer and could then be gradually delivered. The decomposition temperature at which 50% of the material was decomposed ($TD^{50\%}$) was centered at approximately 200 to 250°C, which is indicative of a qualitative measure of the strength of the interaction between the polymer and the small molecule. Notably, the T_m values of the small molecules in the blend were weakly detected in the TGA/DTG profiles, irrespective of the composition. Nevertheless, shifts in the degradation profiles with changes in composition were observed, which suggests that an important interaction occurs between the polymer and the small molecules; on the basis of this result, PEAM and the drugs were assumed to be compatible or partially compatible.

FT-IR Analysis

The FT-IR spectra of the pure components and blends provide information complements the thermal analysis results, which supports our hypothesis concerning interactions in the different polymer mixtures. Specific interactions between components are readily evident through band displacement, intensity changes, broadening of the signals, etc.[17–20] In the case of pure PEAM, the amide-I absorption band at 1644 cm^{-1} and the —NH stretching band between 3300 and 3500 cm^{-1} are frequently used to detect band displacements related to amides. This signal

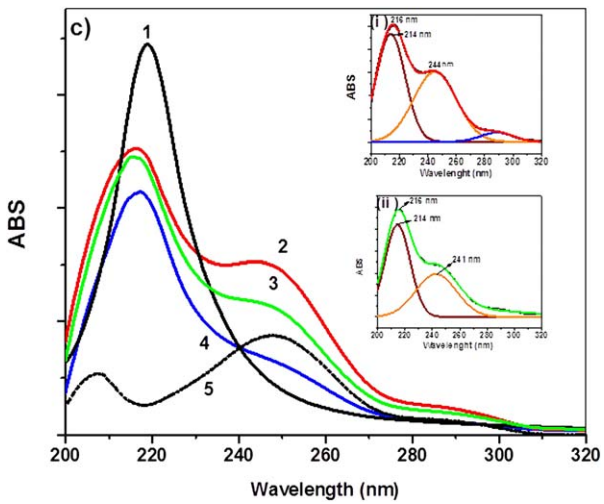

Figure 3. Absorption spectra of: a) PEAM/IBU: (1) PEAM, 0.1 mg/mL, (2) PEAM/IBU 20/80, (3) PEAM/IBU 40/60, (4) PEAM/IBU 50/50, (5) IBU 0.01 mg/mL; b) PEAM/DCF: (1) PEAM, 0.1 mg/mL, (2) PEAM/DCF 20/80, (3) PEAM/DCF 40/60, (4) PEAM/DCF 50/50, (5) DCF 0,01 mg/mL; c) PEAM/PCM: (1) PEAM, 0.1 mg/mL, (2) PEAM/PCM 20/80, (3) PEAM/PCM 40/60, (4) PEAM/PCM 50/50, (5) PCM 0.01 mg/mL. Black (dotted), drug; red, 20 wt %; green, 40 wt %; blue, 50 wt %; black, PEAM. [Color figure can be viewed in the online issue, which is available at wileyonlinelibrary.com.]

Table III. UV-Vis Wavelength Maxima for Blends of PEAM/IBU, PEAM/DCF, and PEAM/PCM

	UV-Vis	Wavelength (nm)		
PEAM/IBU	PEAM	218		
	IBU	221		
	PEAM/IBU (20/80)	219		
	PEAM/IBU (40/60)	217		
	PEAM/IBU (50/50)	217		
PEAM/DCF	PEAM	218		
	DCF	216	281	
	PEAM/DCF(20/80)	216	280	
	PEAM/DCF (40/60)	216	280	
	PEAM/DCF (50/50)	217	280	
PEAM/PCM	Normal spectrum		Deconvoluted spectrum	
	PEAM	218		
	PCM	208	247	-
	PEAM/PCM (20/80)	216	243	214-244
	PEAM/PCM (40/60)	216	-	214-241
	PEAM/PCM (50/50)	217	-	216-232

corresponds to a combined mode with contribution of —C═O and —C—N stretching.[21]

Coleman *et al.*[22,23] analyzed amide/ether interactions in which the presence of —C═O and —NH groups led to the formation of an intramolecular hydrogen bond. In the case of the present work, chains are associated and only terminal functional groups of chains are available for specific intermolecular interactions. The FT-IR absorptions of the pure components and blends show some displacements, as evident in Figure 2.

Figure 2 shows a comparison of the FT-IR spectra of some compositions of the different PEAM/drug blends, where a shift in the wavenumber corresponding to the carbonyl of the amide group is evident. Although the displacements are small, they are enough to assume that at least van der Waals type interactions could be invoked. Therefore, these results would indicate some degree of compatibility between the components of the blends and the inclusion of the small molecule inside the cavity of the dendronized polymer.

The —NH band of PEAM in the spectrum of the blend containing IBU shows variations of the wavenumber for 60% and 80% of drug in the mixture; nevertheless, the —C═O signal associated with the polymers does not show substantial variations. The wavenumber for the nonpolar —CH_3 of PEAM exhibits displacements of up to 19 cm^{-1} when the IBU content is 40% wt. The bending absorptions corresponding to the amide groups in blends containing 20, 40, and 50% show important variations; this observation provides further evidence for the occurrence of important and selective interactions in these systems.

In the spectra of PEAM/DCF and PEAM/PCM, the bands associated with —NH, —C═O and nonpolar groups of the polymer do not show important variations. However, in the spectrum of the blend containing 20% wt of PCM, the wavenumber corresponding to the —NH group shows a displacement of 14 cm^{-1}, which is the most important displacements in the spectra of the studied compositions (Table II). In the spectral region of 1300 cm^{-1}, important shifts are observed for blends with DCF, but not for blends containing PCM. Therefore, the interactions involved in these systems depend strongly on the composition, the conformation of the polymer and the trapping capacity of the polymer toward the small molecule. Accordingly, the interaction strength is strongest in the blends containing IBU. The presence of a carboxylic group and easy access to the small molecules inside the dendronized poly(methacrylamide) should give rise to some type of interaction in comparison with the blend containing DCF, whose FT-IR spectrum shows lower peak intensities. A detailed analysis of the FT-IR spectra for the systems under study is therefore necessary.

In the spectrum of PEAM/IBU [Figure 2(a)], two shifts of the signals at 1720 and 1230 cm^{-1} are observed, corresponding to the stretching vibration of —C═O and the bending vibration of —OH of the carboxylic acid present in IBU (Table II).

The greater shift is from 1230 to 1205 cm^{-1}, which occurs in the case of the blend with a 50/50 wt % composition. In contrast, a small shift of the PEAM vibration corresponding to the —C═O stretching of the amide I is observed. This shift is toward lower frequencies and reaches a value of 5 cm^{-1} relative to the corresponding peak in the spectrum of pure PEAM with a 40/60 wt % composition.

In the case of the PEAM/DCF spectrum shown in Figure 2(b), the signal corresponding to the symmetric stretching of the carboxylate anion —COO^- present in DCF shifts. This signal shifts

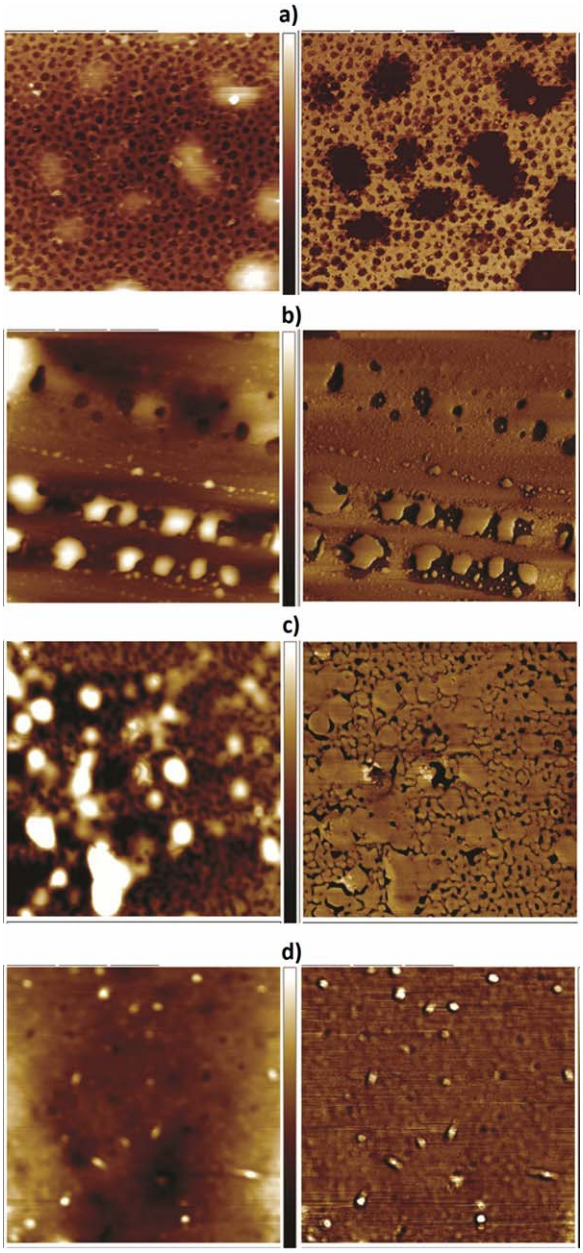

Figure 4. Topography (left) and phase image (right) of films of a) PEAM, b) PEAM/IBU, c) PEAM/DCF 50/50, and d) PEAM/PCM 50/50 (wt %). [Color figure can be viewed in the online issue, which is available at wileyonlinelibrary.com.]

from 1400 to 1390 cm^{-1} when the blend has a 50/50 wt % composition. In the case of this blend, another shift of 5 cm^{-1} corresponding to the stretching vibration of the —C═O of the amide group toward lower frequencies is also observed. In the case of PEAM/PCM [Figure 2(c)], no shifts are observed for the vibrations associated with PCM (Table II).

UV-Vis Spectroscopy

UV-Vis is a powerful tool for detecting interactions between two or more components in a mixture. Any displacement or diminishing of the bands corresponding to the constituents of the blend provides information related to the interactions of the molecules involved in the system.[24–27]

The UV absorption measurements have been used to investigate the interactions between polymers and drugs. Shifts in the maxima or decreases in the absorbance of the bands of the compounds present in the blends correspond to the formation of complex structures. Devarakonda *et al.*[28] have analyzed the complex formation between a dendrimer (PAMAM) and furosemide; the formation of the PAMAM/furosemide complex corresponds to a small shift of approximately 5 nm of the maximum of the band toward lower wavelengths and to the disappearance of a band.[28]

Figure 3 shows a compilation of the absorption profiles for PEAM and blends with the respective drugs. The spectrum of PEAM shows a maximum at 218 nm, and the maximum of the PEAM/IBU blend overlaps that of PEAM, which complicates analysis of the spectra [Figure 3(a)]. However, the peaks of the maxima in the spectra of different compositions show that the observed signal is displaced for PEAM as well as for IBU, which indicates that the constituents are interacting, giving rise to shifts in the absorption bands. Figure 3(b) presents the UV-Vis spectrum of PEAM/DCF, which shows two maxima at 217 and 280 nm. The peak at 217 nm is in the absorption zone of PEAM; therefore, the band at 280 nm was analyzed. No shift in the band corresponding to DCF at different concentrations was detected, consistent with the FT-IR data, where small shifts in the wavenumber for this blend were observed. This lack of shift is attributable to the large size of DCF, which inhibits the generation of stronger interactions. The spectrum of PEAM shows a maximum at 218 nm, and the maximum for PCM occurs at 248 nm [Figure 3(c)]. Changes in the absorbance maximum of PCM were observed, where the maximum shifted from 248 to 243; this shift is evidence of the interaction between PEAM and PCM (Table III). The results suggest that all of the components of the different blends exhibit some extent of compatibility and that these interactions are attributable to specific contacts that arise from the affinity of the functional groups of PEAM and drugs. As a consequence, this procedure of blending small molecules and polymers can be assumed to be a good approach to controlling the release of small molecules from the polymer.

Figure 3(a) presents the absorption spectra for the PEAM/IBU blend. The spectrum of IBU [Figure 3(a-5)] shows a band maximum at 221 nm, whereas the spectra corresponding to the 40/60 [Figure 3(a-3)] and 50/50 [Figure 3(a-4)] blends show a shift of the band maxima toward shorter wavelengths, where the maxima reach a position of 217 nm. The maximum shift is observed when the dendronized polymer and IBU have the same composition, and these shifts are attributed to an interaction between both components of the mixture. In contrast, Figure 3(b) presents the spectra of the PEAM/DCF blend, where the DCF spectrum [Figure 3(b-5)] shows two maxima at 216 and 281 nm. A decrease in intensity of the DCF band at 281 nm is observed for blends of 40/60 and 50/50 wt %, and this decrease is largest in the case of the 50/50 wt % blend [Figure 3(b-4)]. To eliminate the possibility that this decrease in band intensity could be due to dilution, the spectra of the drug

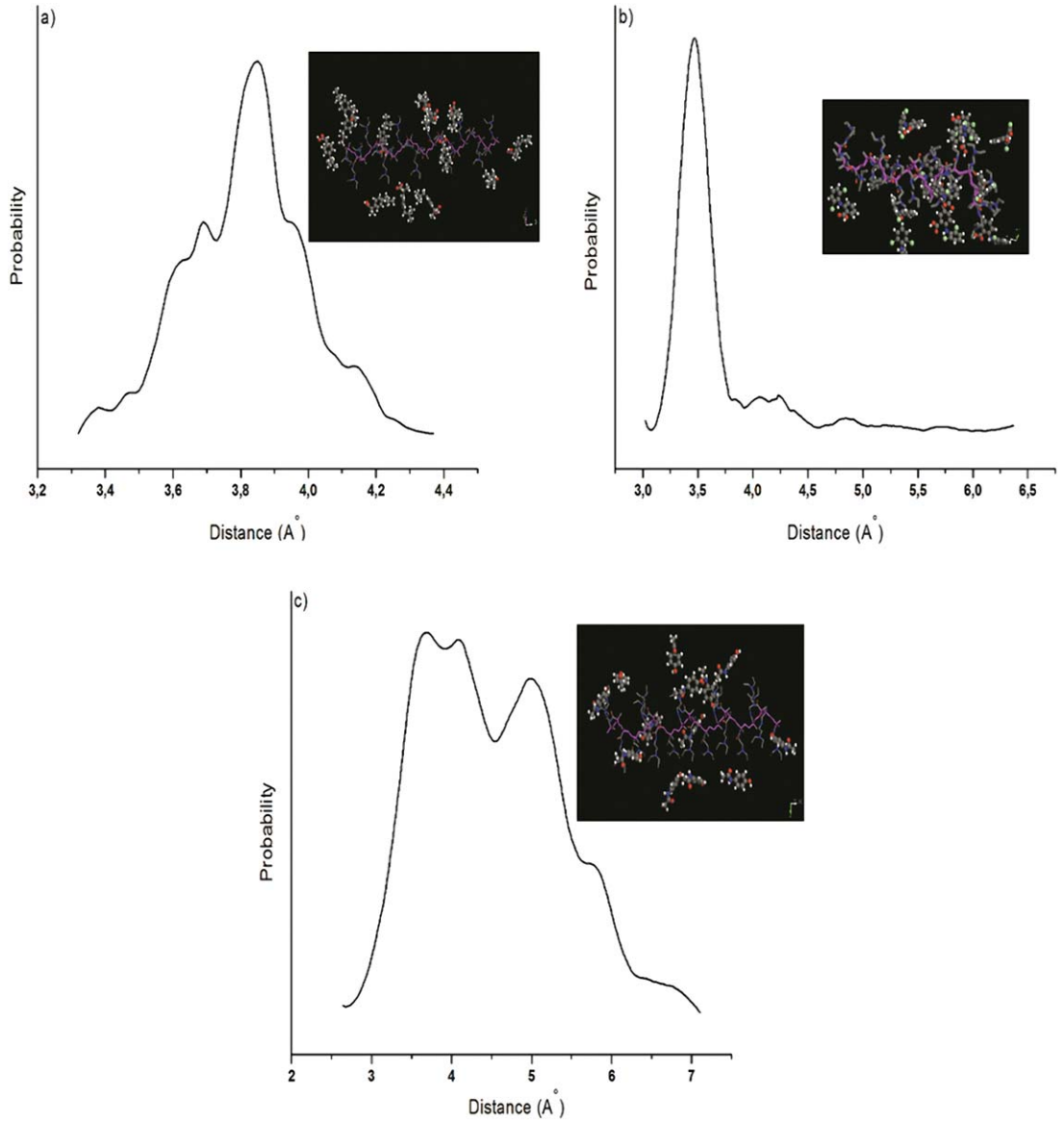

Figure 5. Probability vs. distance plots of PEAM with a) IBU, b) DCF, and c) PCM. [Color figure can be viewed in the online issue, which is available at wileyonlinelibrary.com.]

in each of the three PEAM/DCF blends with different concentrations were compared. For this purpose, a calibration curve for DCF at $\lambda = 281$ nm was constructed, where the correlation coefficient was 0.9798, the intercept was 0.05487, and the molar absorptivity was 1.2966×10^4 L mol^{-1} cm^{-1}. The 20/80 blend was observed to contain the same concentration of the drug indicated by UV-Vis spectrophotometry (spectrum 2). Nevertheless, a difference between the concentrations in the 40/60 and 50/50 blends, e.g., the concentrations in the prepared blends, were 1.16 and 2.3 times greater than the concentrations determined on the basis of the absorbances at λ_{281} in spectra 3 and 4, respectively. The concentration of DCF in the 40/60 blend was determined to be $1.01 \times 10^{-5}M$, whereas that determined using the calibration curve was $8.71 \times 10^{-6}M$. In the case of the 50/50 blend, $5.03 \times 10^{-6}M$ was used in its preparation and the concentration determined using the calibration curve was $2.18 \times 10^{-6}M$. Therefore, the decrease in absorbance of the 281 nm band is attributable to an interaction between the polymer and the drug.

In contrast, Figure 3(c) shows that, for PEAM/PCM, the drug PCM (spectrum 5) exhibits two absorption maxima at 208 and 247 nm, whereas the spectrum for PEAM shows a maximum at 218 nm.

Figure 3(c) presents the UV-Vis spectra for PEAM/PCM; the absorption of PCM [Figure 3(c-5)] shows two maxima at 208 and 247 nm, whereas the spectrum for PEAM [Figure 3(c-1)] shows only one maximum at 218 nm. The spectra of PEAM/PCM with compositions of 20/80 [Figure 3(c-2)] and 40/60 [Figure 3(c-3)] shows one maximum at 216 nm and a shoulder at 245 nm. To better determine the band maxima in the blend spectra, a deconvolution procedure for both spectra was performed. The deconvoluted spectrum [Figure 3(c-i)] for the 20/80 blend

contains two maxima at 214 and 244 nm. The maximum at 214 nm is attributed to a shift of the PEAM band, and the one at 244 nm corresponds to the PCM band in the blend; in contrast, the spectrum deconvoluted [Figure 3(c-ii)] from the spectra for the 40/60 blend shows two maxima at 214 and 241 nm. Therefore, the shift of the PCM band increases with increasing amount of polymer in the blend. Nevertheless, when the composition of the blend is 50/50 wt % [Figure 3(c-4)], the band associated with the drug disappears. All these results lead us to conclude that the dendronized polymer (PEAM) and drugs are compatible.

Atomic Force Microscopy Analysis

AFM was used to analyze the morphologies of the PEAM and blends as another complementary technique for determining the compatibility between the components [28,29] and to verify that interactions occur during the blending process.

Figure 4 shows the AFM images of pure PEAM and the PEAM/IBU, PEAM/DCF, and PEAM/PCM blends, represented as topography and phase images. The image of PEAM shows different zones and imperfections, which may result from the segregation induced by the interactions among the chains of the polymer, as previously indicated by the thermal and infrared analyses. With respect to the PEAM/drug blends, a flat featureless surface is evident, unlike the surface of pure PEAM. The adhesion with the substrate was apparently improved, resulting in a regular thin film. This change in adhesion and surface roughness could be due to the interactions among polymers, resulting in a smooth surface that differs from that of pure PEAM. We also observed hard zones that correspond to the presence of drugs, which appear as bright points. These images suggest that interactions occur among the components of the blend; however, some irregularities are also evident. Topography and phase images for films of PEAM/IBU and PEAM/DCF blends, presented in Figure 4, show that the surface morphology changed again, resulting in a more irregular surface but also resulting in good adhesion with the substrate, probably due to interactions among the polymer/drug system, which could change the surface tension of the film. The images suggest the presence of aggregates of the small molecules on the polymer surface. However, the PEAM/PCM images shows some imperfections but with more homogeneity than those containing IBU and DCF. A surface with some aggregates and irregularities is observed; however, the size of these aggregates is smaller. This result is in good agreement with the previously discussed FT-IR analysis results.

Molecular Dynamics Simulations

To provide further evidence of a specific and detailed view of the mechanism and/or the structural arrangement related to the compatibility among small molecules and PEAM, MD simulation studies were performed. The probability of the distance between PEAM and the small molecules was calculated for all of the blends under investigation: PEAM/IBU, PEAM/DCF, and PEAM/PCM.

Figure 5 shows the plots obtained for each of the blends. The most likely distance between the small molecules was 3.6 Å. This value provides an approximation of the interactions between the polymer and the small molecules, and the magnitude of this value is not sufficient to give rise to hydrogen bond interactions. Hydrophobic interactions likely occur, consistent with the DSC, TGA, FT-IR, and AFM results.

According to the images and the simulated distance among the small molecules and PEAM, van der Waals interactions could be responsible for the compatibility. In the case of blends containing DCF, weak interactions were detected that were attributable to the large size of DCF, which leads to steric hindrance and precludes an accurate approximation of the interactions among the constituents of the blends. The snapshots represented in Figure 5 confirm this assumption and can be considered as a good representation of the macroscopic shape of the mixture.

CONCLUSIONS

Blends of PEAM with drugs were characterized using different experimental techniques to analyze their compatibility behavior. DSC results showed a single T_g value for PEAM/drug blends, which suggested that the components of the mixture were compatible. Thermogravimetric profiles suggested a similar conclusion and indicated that the blends exhibited high thermal stability. FT-IR and UV-Vis spectra confirmed the interactions between the polymer and the drugs, where the shifts of the absorption bands reflected the affinity between the constituents. Interactions between the polymer and small molecules were observed to be quite weak. The bulkiness of the small molecules appeared be a factor that must be considered to explain the interactions among PEAM and drugs. The distances among the constituents of the blends gave rise to a picture about the proximity of the molecules, and these results were in agreement with the data obtained using other different experimental techniques. Nevertheless, the distances obtained were not sufficiently small to result in the generation of hydrogen bond interactions. Finally, the compatibility in these systems was deduced to be governed by hydrophobic interactions, similar to the conclusion derived from the results of DSC measurements.

ACKNOWLEDGMENTS

D.R. and A.L. thank Fondecyt Grant 1120091 for partial financial support. N.A. thanks CONICYT for a doctoral fellowship and project AT-24110036 for doctoral help. I.F thanks Fondecyt Postdoctoral project 3120170. L.G. thanks Universidad de Tarapacá for invaluable help. C.S thank Proyecto Anillo Cientifico ACT 1107. G.K and A.E. thank Basque Government in the frame of Grupos Consolidados (IT-776-13).

REFERENCES

1. Roeser, J.; Moingeon, F.; Heinrich, B.; Masson, P.; Arnaud-Neu, F.; Rawiso, M.; Méry, S. *Macromolecules* **2011**, *44*, 8925.
2. Gunkel, G.; Weinhart, M.; Becherer, T.; Haag, R.; Huck, W. *Biomacromolecules* **2011**, *12*, 4169.
3. Grebikova, L.; Maroni, P.; Muresan, L.; Zhang, B.; Schluüter, A.; Borkovec, M. *Macromolecules* **2013**, *46*, 3603.
4. Gupta, S.; Schade, B.; Kumar, S.; Böttcher, C.; Sharma, S.; Haag, R. *Small* **2013**, *9*, 894.

5. Wang, Y.; Grayson, S. *Adv. Drug Deliver. Rev.* **2012**, *64*, 852.
6. Carlmark, A.; Malmstrom, A.; Malkoch, M. *Chem. Soc. Rev.* **2013**, *42*, 5858.
7. Venkataraman, S.; Hedrick, J.; Yuin Ong, Z. Y.; Yang, C.; Ee, P. L. R.; Hammond, P.; Yang, Y. Y. *Adv. Drug Deliver. Rev.* **2011**, *63*, 1228.
8. Yu, Y.; Chen, C. -K.; Law, W. -C.; Mok, J.; Zou, J.; Prasad, P. N.; Cheng, C. *Mol. Pharmaceutics* **2013**, *10*, 867.
9. She, W.; Li, N.; Luo, K.; Guo, C.; Wang, G.; Geng, Y.; Gu, Z. *Biomaterials* **2013**, *34*, 2252.
10. Wijagkanalan, W.; Kawakami, S.; Hashida, M. *Pharm Res.* **2011**, *28*, 1500.
11. Zeng, H.; Little, H.; Tiambeng, T.; Williams, G.; Guan, Z. *J. Am. Chem. Soc.* **2013**, *135*, 4962.
12. Robeson, L. Polymer Blends: A Comprehensive Review; Hanser, Munich, Cincinnati, **2007**; p 256.
13. Alvarado, N.; Alegría, L.; Sandoval, C.; Kortaberría, G.; Leiva, A.; Gargallo, L.; Radić, D. *J. Macromol. Sci. Part A: Pure Appl. Chem.* **2014**, *51*, 864.
14. Zhang, H.; Fang, J.; Ge, H.; Han, L.; Wang, X.; Hao, Y.; Han, Ch.; Dong, L. *Polym. Eng. Sci.* **2013**, *53*, 112.
15. Garay, M. T.; Alava, C.; Rodríguez, M. *Polymer* **2000**, *41*, 5799.
16. Cesteros, L.; Meaurio, E.; Katime, I. *Polym. Int.* **1994**, *34*, 97.
17. Coleman, M. M.; Painter, P. C. *Prog. Polym. Sci.* **1995**, *20*, 1.
18. Kwei, T.; Pearce, E.; Ren, F.; Chen, J. *J. Polym. Sci. Part B: Polym. Phys.* **1986**, *24*, 1597.
19. Moskala, E. J.; Howe, S. E.; Painter, S. E.; Coleman, M. M. *Macromolecules* **1984**, *17*, 1671.
20. Cesteros, L. *Rev. Iber. Polím.* **2004**, *5*, 111.
21. Chalapathi, V. V.; Ramiah, K. V. *Curr. Sci.* **1986**, *37*, 453.
22. Coleman, M. M.; Skrovanek, D. J.; Hu, J.; Painter, P. C. *Macromolecules* **1988**, *21*, 59.
23. Coleman, M. M.; Lee, H. K.; Skrovanek, D. J.; Painter, P. C. *Macromolecules* **1986**, *19*, 2149.
24. Devarakonda, B.; Otto, D.; Judefeind, A.; Hill, R.; de Villiers, M. *Int. Journal Pharm.* **2007**, *345*, 142.
25. Sahu, A.; Kasoju, N.; Goswami, P.; Bora, U. *J. Biomater. Appl.* **2011**, *25*, 619.
26. Rana, N.; Choi, M.; Kong, J.; Kim, G.; Kim, M.; Kim, S. *Macromol. Mater. Eng.* **2011**, *296*, 131.
27. Syrett, J.; Haddleton, D.; Whittaker, M.; Davis, T.; Boyer, C. *Chem. Commun.* **2011**, *47*, 1449.
28. Devarakonda, B.; Otto, D. P.; Judefeind, A.; Hill, R. A.; de Villiers, M. M. *Int. J. Pharmaceutics* **2007**, *345*,142.
29. Hernández-Montero, N.; Ugartemendia, J. M.; Amestoy, H.; Sarasua, J. R. *J. Polym. Sci. Part B: Polym. Phys.* **2014**, *52*, 111.